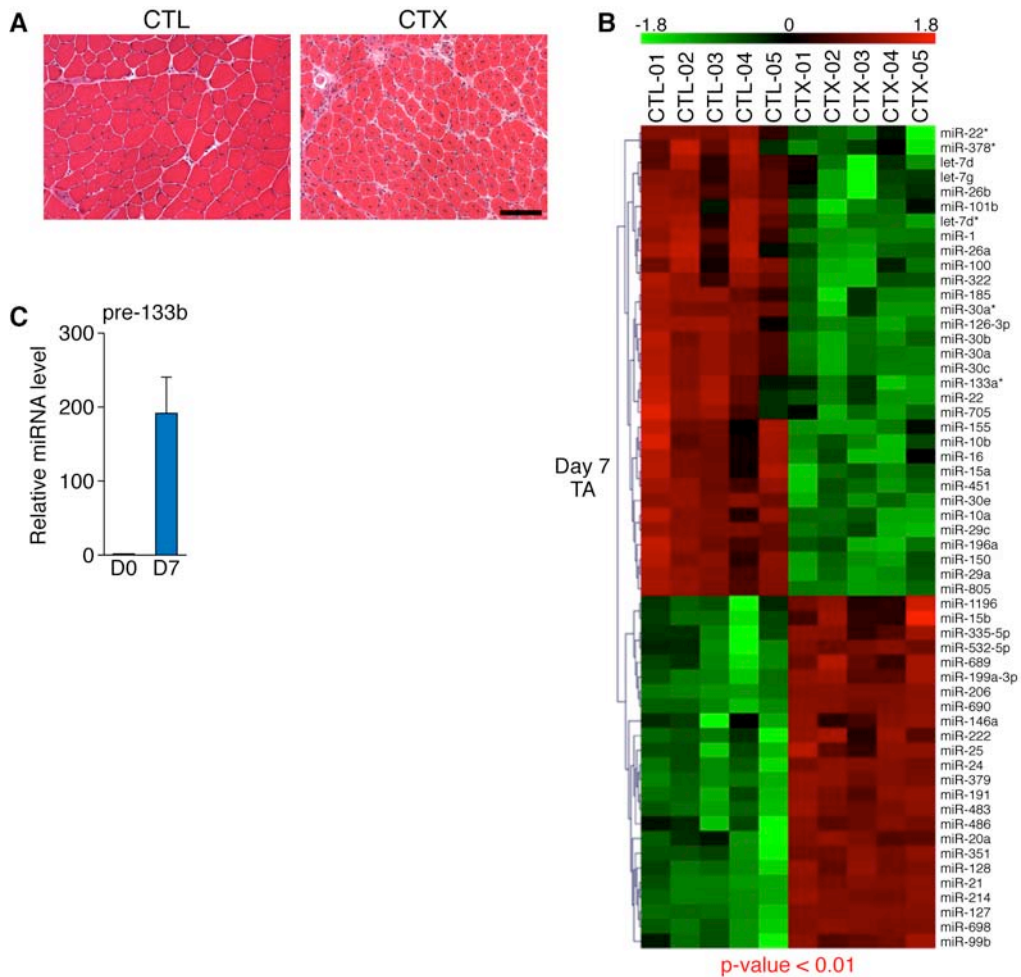
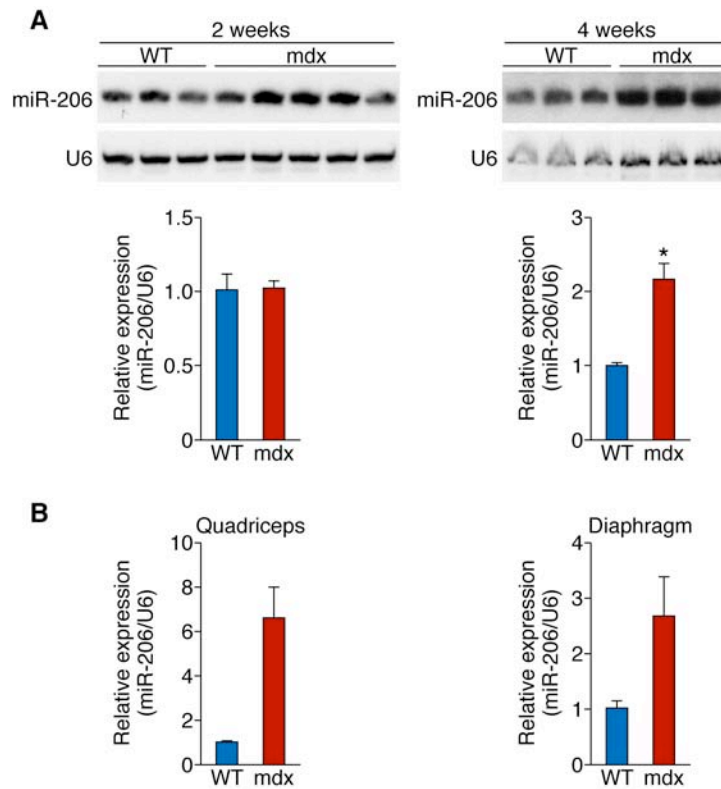


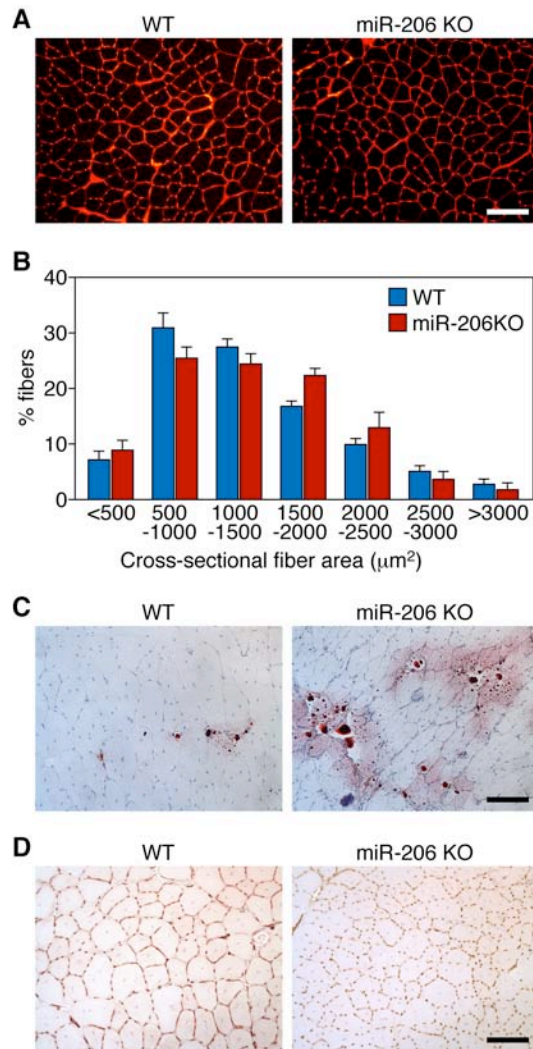
Supplemental Figures



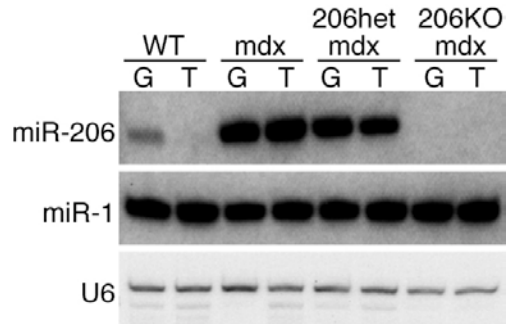
Supplemental Figure 1. microRNA expression profile upon cardiotoxin injury of TA muscle. (A) Hematoxylin and eosin (H&E) staining of transverse sections of TA muscle injected with cardiotoxin (CTX) shows newly formed myofibers with centralized nuclei 7 days post-injury, compared to uninjured contralateral (CTL) TA muscle. Size bar: 100 μm . (B) Heatmap showing miRNA microarray analysis of CTL vs. CTX-injured TA muscle on day 7 post-injury. (C) Expression of pre-miR-133b stem loop in CTX muscle relative to CTL muscle on day 7 post-injury is determined by real-time RT-PCR.



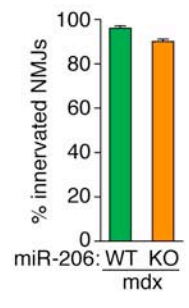
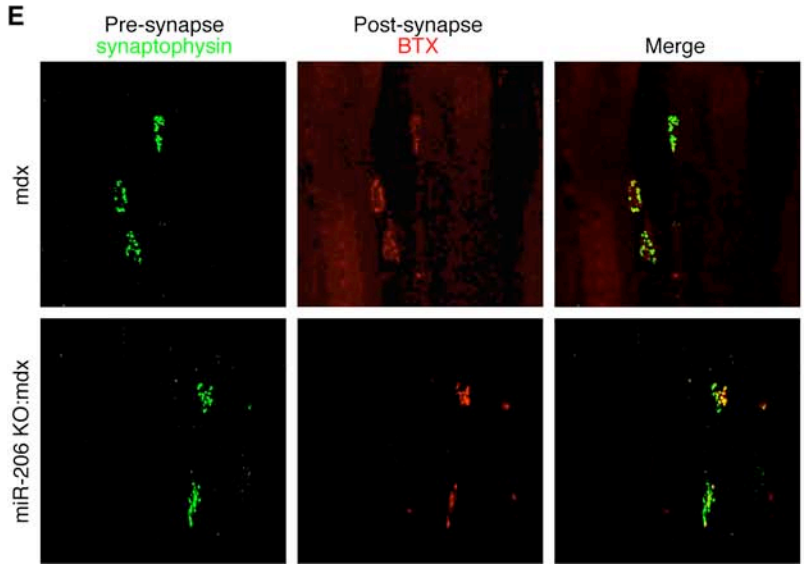
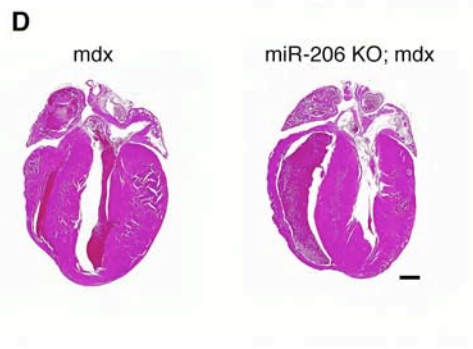
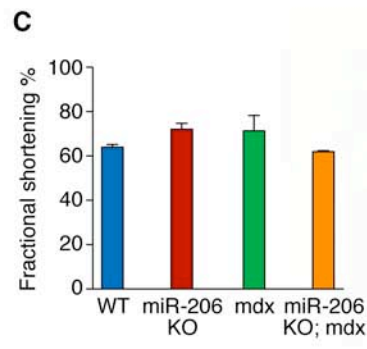
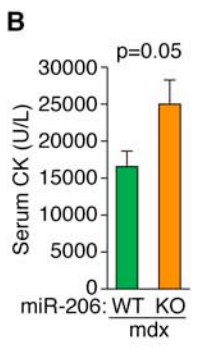
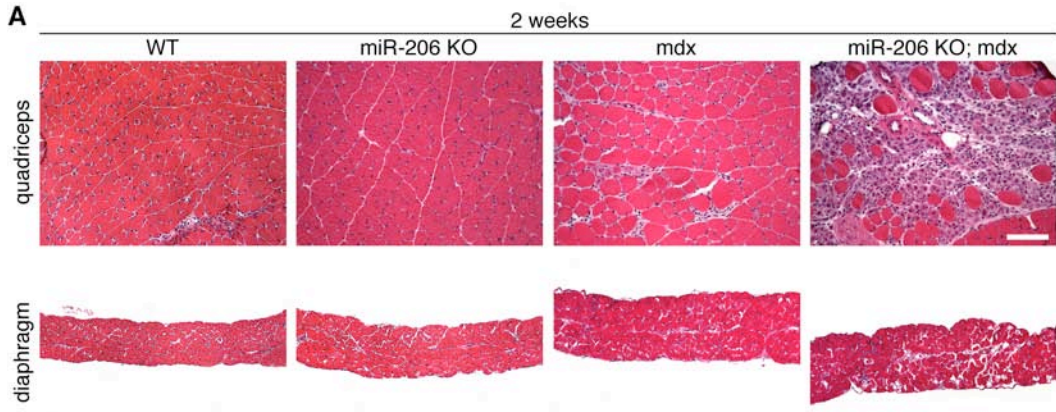
Supplemental Figure 2. Expression of miRNAs in WT and *mdx* mice at different ages. (A) Northern blot analysis (top panel) and real-time RT-PCR (bottom panel) reveal miR-206 expression in quadriceps muscle of WT and *mdx* mice at 2- and 4-weeks of age. (B) Real-time PCR of miR-206 expression in quadriceps and diaphragm muscle of WT and *mdx* mice at 3 months of age.



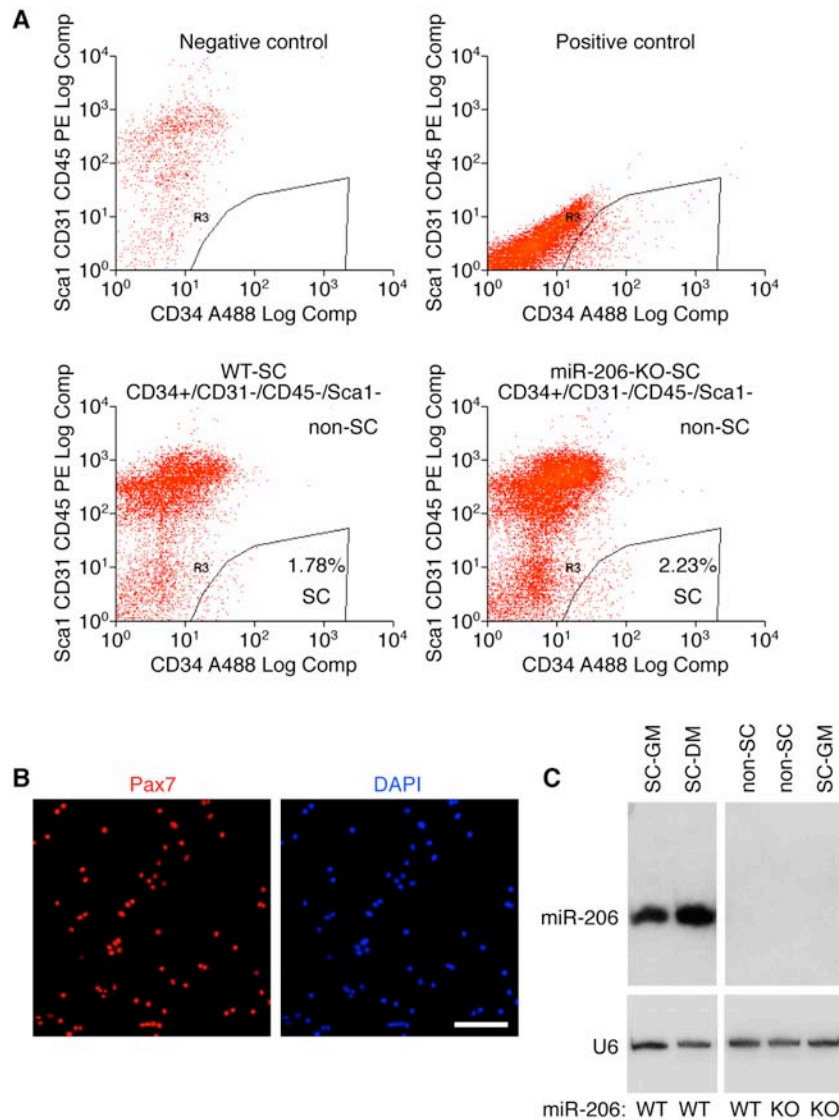
Supplemental Figure 3. Analysis of WT and miR-206 KO TA muscle under normal conditions. (A) Wheat germ agglutinin (WGA) staining of the transverse sections of WT and miR-206 KO TA myofibers. Size bar: 100 μm (B) Cross sectional fiber areas of WT and miR-206 KO TA myofibers were measured by ImageJ based on WGA staining. Five mice from each genotype were analyzed. (C) Oil red O staining of transverse sections of WT and miR-206 KO TA muscle on day 30 after CTX injection. Fatty infiltration is shown in red. Size bar: 100 μm . (D) PECAM1 staining of WT and miR-206 KO TA muscle on day 30 after CTX injection. Capillaries surrounding myofibers are shown as brown dots. Size bar: 100 μm .



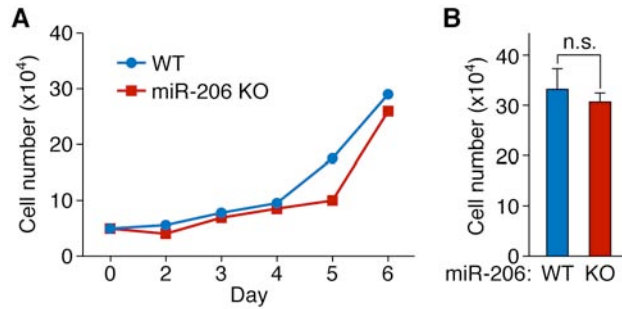
Supplemental Figure 4. Generation of miR-206 KO; *mdx* mice. Northern blot analysis showing the absence of miR-206 in miR-206 KO; *mdx* mice. Expression of miR-1 and U6 are also shown by Northern blot. G, gastrocnemius; T, TA.



Supplemental Figure 5. Histological analysis of WT, miR-206-KO, *mdx*, and miR-206-KO; *mdx* mice. (A) H&E staining of quadriceps and diaphragm muscles at 2 weeks of age. Among 10 miR-206 KO; *mdx* mice analyzed at 2 weeks of age, only 2 displayed severe dystrophic phenotypes. Size bar: 100 μ m. (B) Serum creatine kinase (CK) levels of WT, miR-206 KO; *mdx*, and miR-206 KO; *mdx* mice at 5 months of age. Five mice were analyzed from each genotype. (C) Analysis of cardiac function by echocardiography on WT, miR-206 KO, *mdx*, and miR-206 KO; *mdx* mice at 3 months of age. (D) Histological sections of hearts of *mdx*, and miR-206 KO; *mdx* mice at 3 months of age. Size bar: 1 mm. (E) Analysis of neuromuscular junctions (NMJs) in *mdx* and miR-206 KO; *mdx* mice by immunostaining for synaptophysin (a pre-synapse marker) and α -bungarotoxin (BTX, a post-synapse marker). Percentage of innervated NMJs were counted for 3 mice from each genotype.

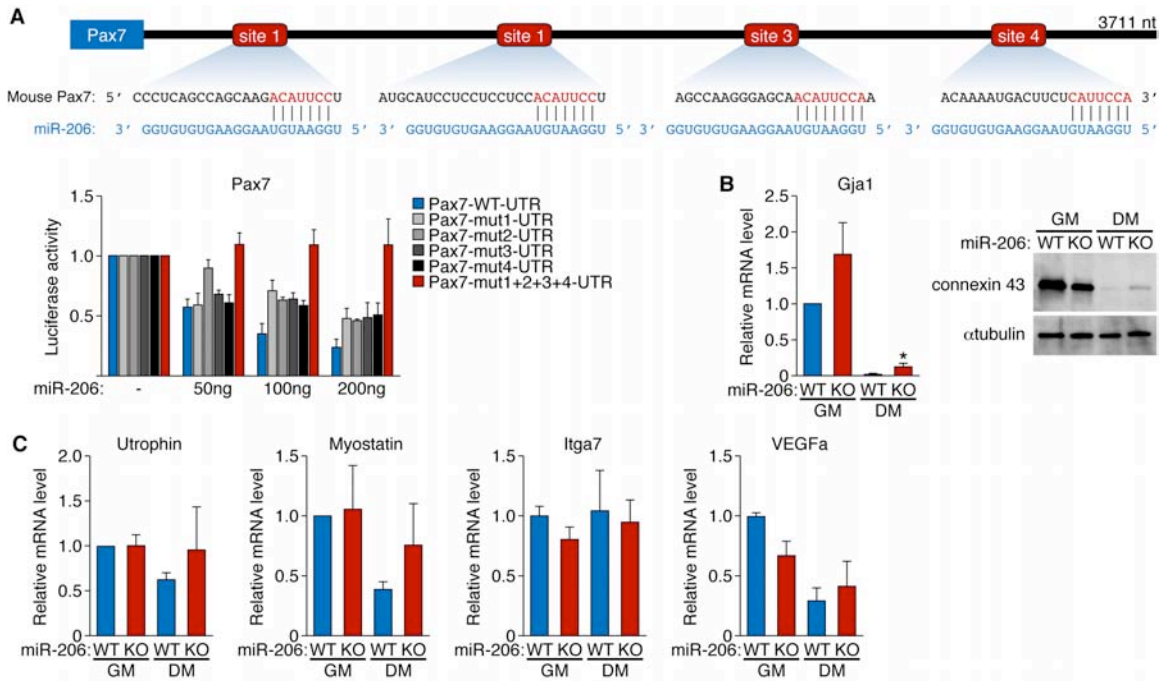


Supplemental Figure 6. FACS sorting of activated satellite cells in WT and miR-206 KO mice. (A) FACS plots of negative control cells (PE-conjugated Sca1⁺CD31⁺CD45⁺) and positive control cells (Alexa 488-conjugated CD34⁺) are shown in top panels. FACS plots of WT and miR-206 KO satellite cells are shown in bottom panels. CD34⁺Sca1⁻CD31⁻CD45⁻ cells were collected as activated satellite cells. There is no significant difference in the percentage of activated satellite cells between WT and miR-206 KO mice. SC: satellite cells; Non-SC: non satellite cells. (B) Immunostaining of Pax7 in WT FACS-sorted satellite cells. Size bar: 100 μ m. (C) Northern blot analysis reveals strong activation of miR-206 in differentiated satellite cells. miR-206 is not expressed in non-SC in WT mice.



Supplemental Figure 7. Proliferation assays for WT and miR-206 KO satellite cells.

(A) Growth curve of WT and miR-206 KO satellite cells. (B) WT and miR-206 KO satellite cells (1×10^5) were plated, grown for 72 hours and counted. The number represents the average of 3 independent experiments ($n=6$ in each experiments). n.s.: not significant.



Supplemental Figure 8. miR-206 represses Pax7 and Gja1 expression. (A) miR-206 represses mouse Pax7 3' UTR in luciferase reporter assay. Watson-Crick base pairings between miR-206 seed sequence and 4 putative miR-206 binding sites in mouse Pax7 3' UTR are shown. miR-206 represses Pax7 3' UTR in luciferase reporter assay and the repression is abolished when all four binding sites are mutated. (B) Gja1 (connexin 43) mRNA and protein levels are upregulated in miR-206 KO satellite cells under differentiation conditions. (C) Real-time RT-PCR reveals expression of utrophin, myostatin, Itga7, and VEGFa mRNA in WT and miR-206 KO satellite cells under growth and differentiation conditions.